

# Protective effect of *Gastrodia elata* Blume in a *Caenorhabditis elegans* model of Alzheimer's disease based on network pharmacology

XIONGFEI SHI, YUAN LUO, LIPING YANG and XIAOHUA DUAN

Yunnan Key Laboratory of Dai and Yi Medicines, Yunnan University of Chinese Medicine, Kunming, Yunnan 650500, P.R. China

Received October 11, 2022; Accepted March 29, 2023

DOI: 10.3892/br.2023.1620

**Abstract.** The aim of the present study was to investigate the protective effect of *Gastrodia elata* Blume (GEB) against *Caenorhabditis elegans* (*C. elegans*) in Alzheimer's disease (AD) through network pharmacology. Firstly, the active constituents of GEB through ETCM and BATMAN-TCM databases were collected and its potential AD-related targets in Swiss Target Prediction were predicted. The potential targets related to AD were collected from the GeneCards, OMIM, CTD and DisGeNET databases, and the differential genes (DEGs) between the normal population and the AD patient population in GSE5281 chip of the Gene Expression Omnibus database were collected at the same time. The intersection of the three targets yielded 59 key targets of GEB for the treatment of AD. The drug-active ingredient-target-AD network diagram was constructed and visualized with Cytoscape software to obtain the core components. Subsequently, protein-protein interaction analysis (PPI) was performed on 59 key targets through STRING database, and Gene Ontology and Kyoto Encyclopedia of Genes and Genomes analyses was performed on 59 key targets. Finally, molecular docking was conducted between core components and core targets using AutoDock software, and the *C. elegans* AD model was used for experimental verification to explore the regulatory paralysis effect of core components on the *C. elegans* model,  $\beta$ -amyloid ( $\beta$ ) plaque deposition, and quantitative polymerase chain reaction verification of the regulatory effect of components on targets. The GEB components 4,4'-dihydroxydiphenyl methane (DM) and protocatechuic aldehyde (PA) were found to be most strongly associated with AD, and five core targets were identified in the PPI network, including GAPDH, EP300,

HSP90AB1, KDM6B, and CREBBP. In addition to GAPDH, the other four targets were successfully docked with DM and PA using AutoDock software. Compared with the control group, 0.5 mM DM and 0.25 mM PA significantly delayed *C. elegans* paralysis ( $P < 0.01$ ), and inhibited the aggregation of  $A\beta$  plaques in *C. elegans*. Both DM and PA could upregulate the expression level of core target gene HSP90AB1 ( $P < 0.01$ ), and DM upregulated the expression of KDM6B ( $P < 0.01$ ), suggesting that DM and PA may be potential active components of GEB in the treatment of AD.

## Introduction

Alzheimer's disease (AD) is a dementia with a complex pathogenesis. It is a slowly progressing neurodegenerative disease, with clinical manifestations including progressive memory loss, language and intellectual impairment, and the inability to take care of oneself. It is estimated that the number of patients with AD will exceed 78 million worldwide, in 2030 (World Alzheimer Report 2021; <https://www.alzint.org/resource/world-alzheimer-report-2021/>). The presence of extracellular  $\beta$ -amyloid ( $A\beta$ ) deposits and the intracellular accumulation of hyperphosphorylated tau are still the main neuropathological criteria for the diagnosis of AD (1,2). Although significant progress has been made in elucidating the key pathogenetic mechanisms, the etiopathogenesis of AD is far from clear. Alternative medicines based on natural herbs have garnered attention in recent years due to their abundance, diversity, low toxicity, effectiveness, and low cost. Chinese herbal medicines with a wide range of pharmacological activities have become prospective interventions for the prevention and treatment of human diseases (3).

Tianma [*Gastrodia elata* Blume, (GEB)] is an exceptional traditional herb. The GEB dry tuber is featured in the 2015 edition of the Chinese Pharmacopoeia (4). Recent studies have revealed that GEB and its active components have diverse pharmacological effects on Parkinson's disease (5), AD (6,7), and improving ischemia-reperfusion injury (8). The water extract of GEB can be used as a food additive to promote the neuroregenerative process (9). It inhibits the production of stress-related proteins and activates the neuroprotective genes in humans (10). GEB also controls chaperone/proteasome

---

Correspondence to: Dr Xiaohua Duan, Yunnan Key Laboratory of Dai and Yi Medicines, Yunnan University of Chinese Medicine, 1076 Yuhua Road, Chenggong, Kunming, Yunnan 650500, P.R. China  
E-mail: 1047896527@qq.com

**Key words:** *Gastrodia*, Alzheimer disease, network pharmacology, pharmacological mechanism, *Caenorhabditis elegans*

degradation pathways in SH-SY5Y cells, such as the production of CALR and HSP70/90 proteins, to enhance synapse regeneration, thereby playing a role in neuroprotection (11). Gastrodin, the major bioactive component in GEB, was demonstrated to ameliorate memory deficits in mice by inhibiting the expression of  $\beta$ -site APP-cleaving enzyme 1 (BACE1) protein and reducing the levels of eIF2 $\alpha$  and phosphorylated PKR in cells (12). Furthermore, gastrodin significantly improved cell viability in a cell culture model of AD induced by A $\beta$ 25-35 and reduced the release of lactate dehydrogenase (LDH), thereby protecting neurons from A $\beta$  toxicity (13). p-Hydroxybenzyl alcohol is another key component in GEB. p-Hydroxybenzyl alcohol was revealed to reduce the accumulation of reactive oxygen species in *Caenorhabditis elegans* (*C. elegans*) and decrease A $\beta$  plaque deposition (14). There are numerous studies on GEB and its active components (15,16), however the underlying mechanisms of action remain unclear due to the complexity of bioactive compounds in traditional Chinese medicine (TCM). It is therefore necessary to further study the therapeutic potential of GEB in AD.

Network pharmacology is a useful tool for identifying the bioactive substances in TCM formulations. It can also reveal the mechanisms that underlie the effects of TCM (17) and provide insight into the overall regulatory mechanism of the 'component-target-pathway'. Using the network pharmacology approach, numerous studies have successfully investigated the mechanisms of action of active components in various Chinese herbal medicines, and have identified drugs with the potential to treat diseases. For example, Yizhiqingxin formula may exert its neuroprotective effect in AD via the PI3K/Akt signaling pathway. Polygonatine A, polygonatine C and 4',5-dihydroxyflavone were demonstrated to significantly increase the survival rate and calcium levels in a PC12 cell model of amyloid  $\beta$  toxicity, and exhibited potential in preventing and treating AD (18,19). Network pharmacology has been gradually applied to the study of TCM components. Whole-formula, multi-component and multi-target analyses can help optimize compound prescription, according to the tenets of TCM (20). The Gene Expression Omnibus (GEO) is a global database of high-quality gene expression data, with expansive information on gene expression profiles, including significant differences in expression between diseased tissues and normal tissues (18). Therefore, in the present study, network pharmacology was combined with the GEO database to investigate the mechanism of action of GEB in the treatment of AD.

A component-target-gene network was first constructed to explore the underlying molecular mechanisms. The core network and targets of GEB were then identified using a protein-protein interaction (PPI) network, and the key pathways were clarified using Gene Ontology (GO) and Kyoto Encyclopedia of Genes and Genomes (KEGG) enrichment analyses. Finally, molecular docking and reverse transcription-quantitative polymerase chain reaction (RT-qPCR) experiments were used to verify the association between key targets and components.

## Materials and methods

### Network pharmacology analysis

**Analysis of active components.** The active components of GEB were obtained by searching for 'TIAN MA' or '*Gastrodia elata*

BI' in the Encyclopedia of Traditional Chinese Medicine (ETCM; <http://www.tcmip.cn/ETCM/index.php/Home/Index/>), Bioinformatics Analysis Tool for Molecular Mechanisms of Traditional Chinese Medicine (BATMAN-TCM; <http://bionet.ncpsb.org.cn/batman-tcm/>) and literature from China National Knowledge Infrastructure (CNKI). Subsequently, using the PubChem database (<http://pubchem.ncbi.nlm.nih.gov/>), the obtained active components were converted to Canonical SMILES format and imported into the SwissTargetPrediction database (<http://swisstargetprediction.ch/>) (21) with species set to 'Homo sapiens' to acquire the targets of the active components of GEB.

**Obtaining gene targets related to AD.** GeneCards (<https://www.genecards.org/>), OMIM (<https://omim.org/>), CTD (<http://ctdbase.org/>) and DisGeNET (<http://www.disgenet.org/>) databases (22,23) were used to screen potential targets associated with AD by searching for the keyword 'Alzheimer disease'. The results from the four databases were integrated and deduplicated for the following analyses.

**Construction of the drug-active component-target-AD network.** Limma (version 3.44.3) (24) R package was used to screen for differential genes (DEGs) between 10 AD and 13 control samples in GSE5281 (18) with  $|\log_2FC| > 1$  and adjusted P-value  $< 0.05$ . The potential therapeutic targets for the anti-AD effects of GEB were obtained by overlapping targets of active components, AD-related targets and DEGs. The drug-active component-target-AD network was then constructed and visualized using Cytoscape software (version 3.2.1) (25).

**Construction of a PPI network.** Next, potential therapeutic targets were input into STRING database (<https://string-db.org>). In order to build a PPI network with a confidence level  $> 0.4$ , Cytoscape software (version 3.2.1) was used to visualize the PPI network and calculate the degree of each node in the PPI network to obtain the core target. Core targets were defined as the top five nodes with the highest degrees. Heat maps were created using the Pheatmap (version 0.7.7) (26) package in R for potential targets.

**GO and KEGG enrichment analyses.** ClusterProfiler (version 3.18.0) (27) R package was used for GO and KEGG enrichment analyses of GEB-AD-related core targets. The GO system contains three main categories including biological process (BP), cellular component (CC) and molecular function (MF). An adjusted P-value of  $< 0.05$  was considered to indicate significant enrichment.

**Molecular docking.** Core targets acting as large molecular receptors, and the corresponding active compounds, acting as small molecule ligands, were selected for molecular docking analysis. The 3D structures of the core targets were downloaded from the PDB database (<https://www.rcsb.org/>). The 2D structures of the corresponding active ingredients were downloaded from the PubChem database (<https://pubchem.ncbi.nlm.nih.gov/>). The raw files of core targets and the corresponding active components were processed with the AutoDock (version 4.2) (28) tool and converted to PDBQT format for molecular docking. Binding activity was expressed

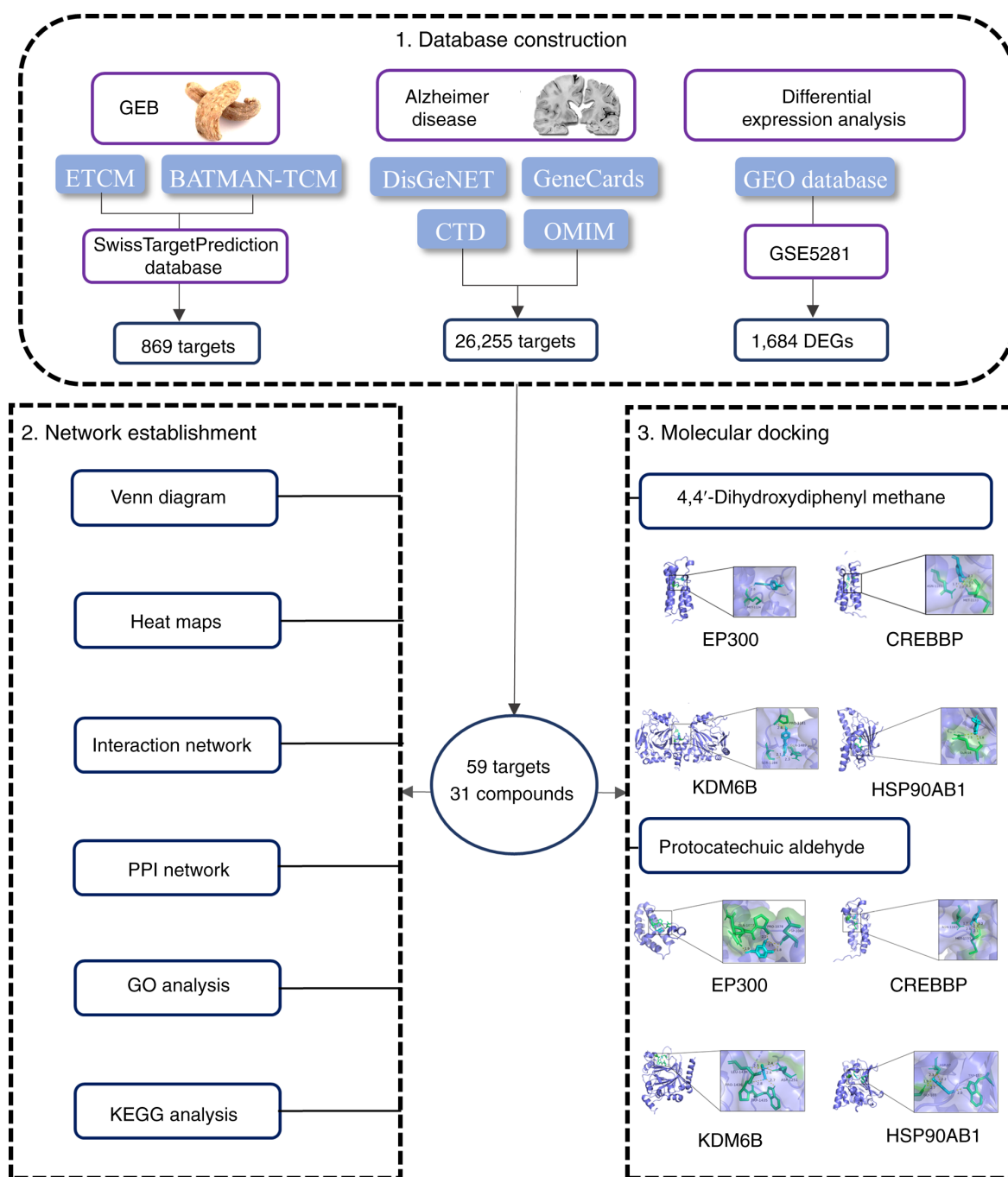


Figure 1. Flowchart of network pharmacology and molecular docking. GEB, *Gastrodia elata* Blume; GEO, Gene Expression Omnibus; ETCM, Encyclopedia of Traditional Chinese Medicine; BATMAN-TCM, Bioinformatics Analysis Tool for Molecular Mechanisms of Traditional Chinese Medicine; CTD, Comparative Toxicogenomics Database; OMIM, Online Mendelian Inheritance in Man; DEGs, differentially expressed genes; PPI, protein-protein interaction; GO, Gene Ontology; KEGG, Kyoto Encyclopedia of Genes and Genomes.

as binding energy; the lower the bonding energy, the more stable the docking module (29). In general, a docking energy <math><-5\text{ kcal/mol}</math> indicates good docking (30).

#### Experimental verification

**Materials.** 4,4'-Dihydroxydiphenyl methane (DM) and protocatechuic aldehyde (PA) were purchased from Chengdu Alfa Biotechnology Co., Ltd. (purity  $\geq 98\%$ ). Other reagents included RNAsimple Total RNA Kit (cat. no. DP419; Tiangen Biotech Co., Ltd.), GoScript™ Reverse Transcription System (cat. no. A5000; Promega Corporation), GoTaq® qPCR Master

Mix (cat. no. A6001; Promega Corporation). Transgenic *C. elegans* strains CL4176 [dvIs27 (*myo-3p::Aβ1-42::let-851* 3'UTR) + *rol-6* (*su1006*)] and CL2006 [dvIs2 (pCL12 (*unc-54*/human Aβ1-42 minigene) + pRF4)], and *Escherichia coli* OP50 were obtained from the Caenorhabditis Genetics Center (CGC) of the University of Minnesota (Minneapolis, USA). The network pharmacology workflow is presented in Fig. 1.

***C. elegans* strains and drug treatment.** The strain CL2006 was propagated at 20°C, and the strain CL4176 was propagated

at 16°C. All *C. elegans* strains were routinely propagated on solid nematode growth medium (NGM; consisting of 300 ml deionized water including 0.82 g peptone, Oxoid Limited; Thermo Fisher Scientific; 1.2 g NaCl, Tianjin Fengchuan Chemical Reagent Co., Ltd.; 5.15 g agar, Beijing Solarbio Science & Technology Co., Ltd.; autoclaved and supplemented 1 mM MgSO<sub>4</sub>, 1 mM CaCl<sub>2</sub>, Tianjin Fengchuan Chemical Reagent Co., Ltd.; 12.9 mM cholesterol solution, MACKLIN) with *E. coli* OP50 as a food source. *C. elegans* was treated with sodium hypochlorite, and synchronized larvae (L1 stage) were obtained after eggs were incubated overnight in M9 buffer (containing 22 mM KH<sub>2</sub>PO<sub>4</sub>, 42 mM Na<sub>2</sub>HPO<sub>4</sub>, autoclaved and supplemented with 1 mM MgSO<sub>4</sub>; all the reagents were from Tianjin Fengchuan Chemical Reagent Co., Ltd.) for experiment. Transgenic *C. elegans* strains CL2006 and CL4176 were used as AD animal models. *C. elegans* were randomly divided into control and drug pretreatment groups. The preparation was dissolved in 0.1% DMSO and diluted with ultrapure water to the appropriate concentration. Based on a previous study (31), various concentrations of DM (0.125, 0.25, 0.5, 1, 2 mM) and PA (0.125, 0.25, 0.5, 1 mM) were used to assess safety and efficacy in *C. elegans*.

**Paralysis assay.** CL4176, a temperature-sensitive transgenic model, has been demonstrated to inactivate the smg-1 system when the temperature increases from 16°C to 25°C, which leads to overexpression of A $\beta$  in muscles and a paralysis phenotype. CL4176 nematodes synchronized to the L1 stage were transferred to 35 mm culture plates with or without OP50 and drugs, cultured at 16°C for 36 h and then at 25°C for transgene induction. After 24 h of culture at 25°C, the paralyzed worms were observed every 2 h. When they could not move or respond to platinum wire stimulation, they were considered paralyzed (32).

**Fluorescence staining of A $\beta$  deposits.** Transgenic CL2006 worms synchronized to the L4 stage (early adult stage) were inoculated on NGM plates with or without drugs, and N2 was used as a negative control for A $\beta$  deposition (32). Following incubation at 20°C for 48 h, the worms were collected with M9 buffer and fixed in 4% paraformaldehyde/PBS (pH 7.4) (cat. no. BL539A; Biosharp Life Sciences) at 4°C for 24 h. The worms were then treated with 5%  $\beta$ -mercaptoethanol (cat. no. M828395; Macklin, Inc.), 1% Triton X-100 (cat. no. MB2486; Dalian Meilun Biology Technology Co., Ltd.) and 125 mM Tris (pH 7.4) (cat. no. T8060; Beijing Solarbio Science & Technology Co., Ltd.) at 37°C for 24 h. The samples were stained with 0.125% thioflavin S (cat. no. S19293; Shanghai Yuanye Bio-Technology Co., Ltd.) in 50% ethanol at room temperature for 2 min, and then with 50% ethanol. The samples were thereafter rinsed and transferred to a glass slide for observation under a laser scanning confocal microscope (LSM900; Carl Zeiss AG). The number of thioflavin S-reactive deposits in the area anterior to the pharyngeal bulb was counted.

**RNA extraction and quantitation.** Synchronized L1 stage CL4176 nematodes were transferred to NGM medium with or without drugs (~500 nematodes in each plate) and cultured at 15°C for 36 h, and then at 25°C for a further 36 h. The worms were collected in an EP tube with M9 buffer, rinsed, and the

supernatant was discarded (33). Total RNA was extracted using RNAsimple Total RNA Kit, and the concentration and purity were measured with an ultra-micro spectrophotometer (SMA6000; Merinton Instrument, Inc.). cDNA was obtained by reverse transcription using GoScript™ Reverse Transcription System and a thermocycler (Veriti Applied Biosystems; Thermo Fisher Scientific, Inc.), and target mRNA was quantified using GoTaq® qPCR Master Mix and real-time PCR (C1000 Touch PCR; Bio-Rad Laboratories, Inc.). Reverse transcription-quantitative polymerase chain reaction (RT-qPCR) was performed under the following operating conditions: 95°C for 10 min, followed by 40 cycles of 95°C for 15 sec, 55°C for 30 sec and 72°C for 30 sec. The reaction was then cooled and maintained at 4°C.  $\beta$ -actin was used as a housekeeping gene. Relative gene expression was calculated using the 2<sup>- $\Delta\Delta C_q$</sup>  method (34), and each reaction was repeated three times. The primers used in this assay are listed in Table SI.

**Statistical analysis.** GraphPad Prism software 8.0 (GraphPad Software, Inc.) was used for statistical analyses. All data are presented as the means  $\pm$  SD. All experiments were repeated three times. Curves were plotted using Kaplan-Meier survival curves and statistical analyses of differences between groups in the paralysis assays were performed using the log-rank test. In addition, unpaired Student's t-test was used to compare differences between two groups. P<0.05 was considered to indicate a statistically significant difference.

## Results

### *Prediction of components and targets based on network pharmacology*

**Analysis of active components.** A total of 21 and 23 active components in GEB were obtained from the ETCM and BATMAN-TCM databases, respectively. After integrating and de-duplicating the data, 34 active components were obtained. After removing three active components (bis(4-hydroxybenzyl)ether mono- $\beta$ -d-glucopyranoside, tris-[4-( $\beta$ -d-glucopyranosyloxy)benzyl]citrate and vanillyl alcohol) with no canonical SMILES format, the remaining 31 active components (Table I) were imported into the SwissTargetPrediction database. A total of 869 targets of the active components of GEB were obtained. By mining the GeneCards, OMIM, CTD and DisGeNET databases, and after removing duplicate data, a total of 26,255 AD-related targets were obtained.

**Obtaining gene targets related to AD.** To obtain more robust AD-related targets, a total of 1,684 DEGs between AD and control samples were identified, among which 975 were upregulated and 709 were downregulated. The red dots represent upregulated genes, the green dots represent downregulated genes, and the gray dots represent genes with no significant difference (Fig. S1). Thereafter, by overlapping 869 targets of the active components of GEB (26,255 AD-related targets and 1,684 DEGs), a total of 59 potential targets of the anti-AD therapeutic effects of GEB were obtained (Fig. 2A and Table SII). The heat map shows the expression of 59 potential therapeutic targets in AD and control samples (Fig. S2). Each square represents a gene. The greater the expression, the darker

Table I. Components of GEB for analysis.

No.	Compounds	Molecular weight	Molecular formula
1	Sitosterol	414.707	C29H50O
2	Vanillin	152.147	C8H8O3
3	20-Hexadecanoylingenol	586.94	C36H58O6
4	4-(4'-Hydroxybenzyloxy)benzyl methyl ether	244.286	C15H16O3
5	4,4'-Dihydroxydiphenyl methane	200.233	C13H12O2
6	4-Ethoxymethylphenyl-4'-hydroxybenzylether	258.312	C16H18O3
7	4-Hydroxybenzyl alcohol	124.137	C7H8O2
8	4-Hydroxybenzyl methyl ether	138.164	C8H10O2
9	4-Hydroxybenzylamine	123.152	C7H9NO
10	7-Hydroxybiopterin	253.22	C9H11N5O4
11	Vanillin acetate	212.2	C10H12O5
12	Bis(4-Hydroxybenzyl)ether	230.259	C14H14O
13	Cetylic Acid	256.42	C16H32O2
14	Citric Acid	192.124	C6H8O7
15	Citronellal	154.249	C10H18O
16	Daucosterol	576.847	C35H60O6
17	Dauricine	624.766	C38H44N2O6
18	Ethoxysanguinarine	377.390	C22H19NO5
19	$\gamma$ -Sitosterol	414.7	C29H50O
20	Gastrodamine	245.274	C14H15NO3
21	Gastrodin	286.278	C13H18O7
22	Gaultheroside A	552.6	C27H36O12
23	M-Hydroxybenzoic acid	138.121	C7H6O3
24	P-Hydroxybenzaldehyde	122.121	C7H6O2
25	P-Hydroxybenzyl alcohol	124.137	C7H8O2
26	P-Hydroxybenzyl ethyl ether	152.190	C9H12O2
27	Protocatechuic aldehyde	138.120	C7H6O3
28	Succinic Acid	118.088	C4H6O4
29	Suchilactone	368.380	C21H20O6
30	Sucrose	342.296	C12H22O11
31	Suffruticoside A	612.5	C27H32O16

GEB, *Gastrodia elata* Blume.

the color (red, upregulated; blue, downregulated). Each row represents the expression of each gene in different samples; the column represents expression of all genes in each sample.

**Construction of the drug-active component-target-AD network.** Based on these results, a drug-active component-target-AD network with 92 nodes (AD, TIANMA, 31 active compounds, and 59 target genes) and 269 edges (Fig. 2B) was constructed. Furthermore, to investigate the interactions of the 59 therapeutic targets of GEB, a PPI network was constructed using the STRING database. The PPI network was composed of 47 nodes and 119 edges, revealing that therapeutic targets had a strong and complex association with each other. The color of the nodes, ranging from blue to purple, indicates the degree, ranging from small to large (Fig. 2C). GAPDH, EP300, HSP90AB1, KDM6B and CREBBP had the highest degrees, and were therefore considered to be core targets and were used for molecular docking analysis.

**GO and KEGG enrichment analyses.** Next, the biological functions of the 59 potential therapeutic targets were explored, which were significantly enriched in the 163 BP, 9 CC, 38 MF and 21 KEGG pathways. The top 10 BP, MF and CC pathways were involved in gene transcription, such as 'histone demethylation', 'histone modification', 'covalent chromatin modification', 'DNA-binding transcription factor binding', 'transcription coactivator activity' and 'NAD binding' (Fig. 3A). The top 10 enriched KEGG pathways were closely associated with neurodegeneration and neuroendocrinology, including the 'cAMP signaling pathway', 'HIF-1 signaling pathway' and 'Glucagon signaling pathway' (Fig. 3B and Table SIII).

**Results of molecular docking.** As mentioned above, GAPDH, EP300, HSP90AB1, KDM6B and CREBBP may be the core potential targets of GEB in the treatment of AD. GAPDH is an internal reference, and was therefore not considered further.

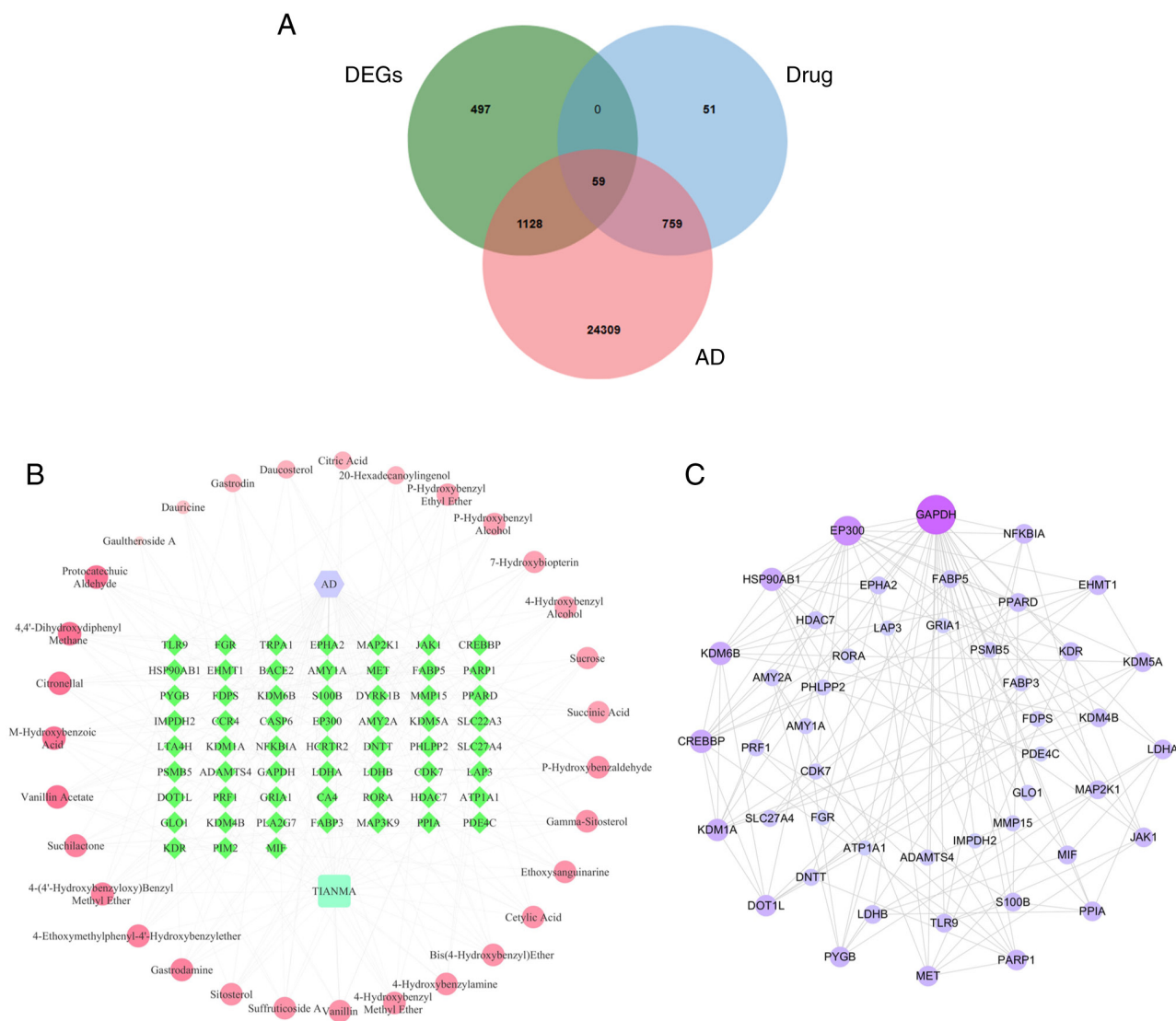


Figure 2. Active components and potential target proteins for GEB. (A) Venn diagram was used to determine the intersection between the GEB and AD targets. (B) Drug-compound-target-AD interaction network. The red circles represent candidate compounds and the green diamonds are targets. The degree value of a node is determined by the number of edges connected to the node. The square represents drug (TIANMA), and the hexagon represents Alzheimer's disease (AD). (C) PPI network. As the value is higher, the circle is larger. DEGs, differential genes; AD, Alzheimer's disease; TIANMA, *Gastrodia elata* Blume.

DM and PA, two components which are at the forefront in the network diagram were investigated. These two components, with high moderate values in the network diagram, were matched with four core protein targets, and their docking potential was studied. The binding energies were between -8.12 and -5.04 kcal/mol (Table II), exhibiting good docking activity (the more negative the value, the stronger the molecular docking). Both compounds interact with the four target proteins mainly through hydrogen bonds.

The results revealed that DM forms a hydrogen bond with MET-1124 on EP300 (Fig. 4A). DM forms five hydrogen bonds with ASN-1163 and MET-1133 on CREBBP (Fig. 4B). DM forms three hydrogen bonds, with GLN-1489, SER-1184 and PRO-1181, on KDM6B (Fig. 4C). DM forms two hydrogen bonds, with GLN-18, on HSP90AB1 (Fig. 4D). PA forms four hydrogen bonds, with GLN-1077, ASP-1080 and PRO-1078, on EP300 (Fig. 4E). PA forms five hydrogen bonds, with ASN-1163 and MET-1133, on CREBBP (Fig. 4F). PA forms five hydrogen bonds, with LEU-1438, ASP-1251, TRP-1435

and PRO-1436, on KDM6B (Fig. 4G). PA forms five hydrogen bonds, with GLY-103, ASP-97 and TRP-157, on HSP90AB1 (Fig. 4H).

#### Effect of GEB on transgenic *C. elegans*

*Effects of DM and PA on paralysis in C. elegans.* DM (0, 0.125, 0.25, 0.5, 1, 2 mM) and PA (0, 0.125, 0.25, 0.5 mM) had no obvious toxicity. When the concentration of DM exceeded 0.5 mM, the effect of delaying *C. elegans* paralysis exhibited a downward trend, and 0.5 mM DM exerted the most marked effect ( $P < 0.01$ ) (Fig. 5A). When the concentration of PA exceeded 0.5 mM, it displayed a toxic effect; a PA concentration of 0.25 mM exhibited the most marked therapeutic effect ( $P < 0.01$ ) (Fig. 5B). Therefore, DM and PA have potential anti-AD activity.

*DM and PA inhibit the deposition of A $\beta$  in transgenic C. elegans.* In order to study the effects of DM and PA on the aggregation of A $\beta$ , the formation of amyloid fibrils was

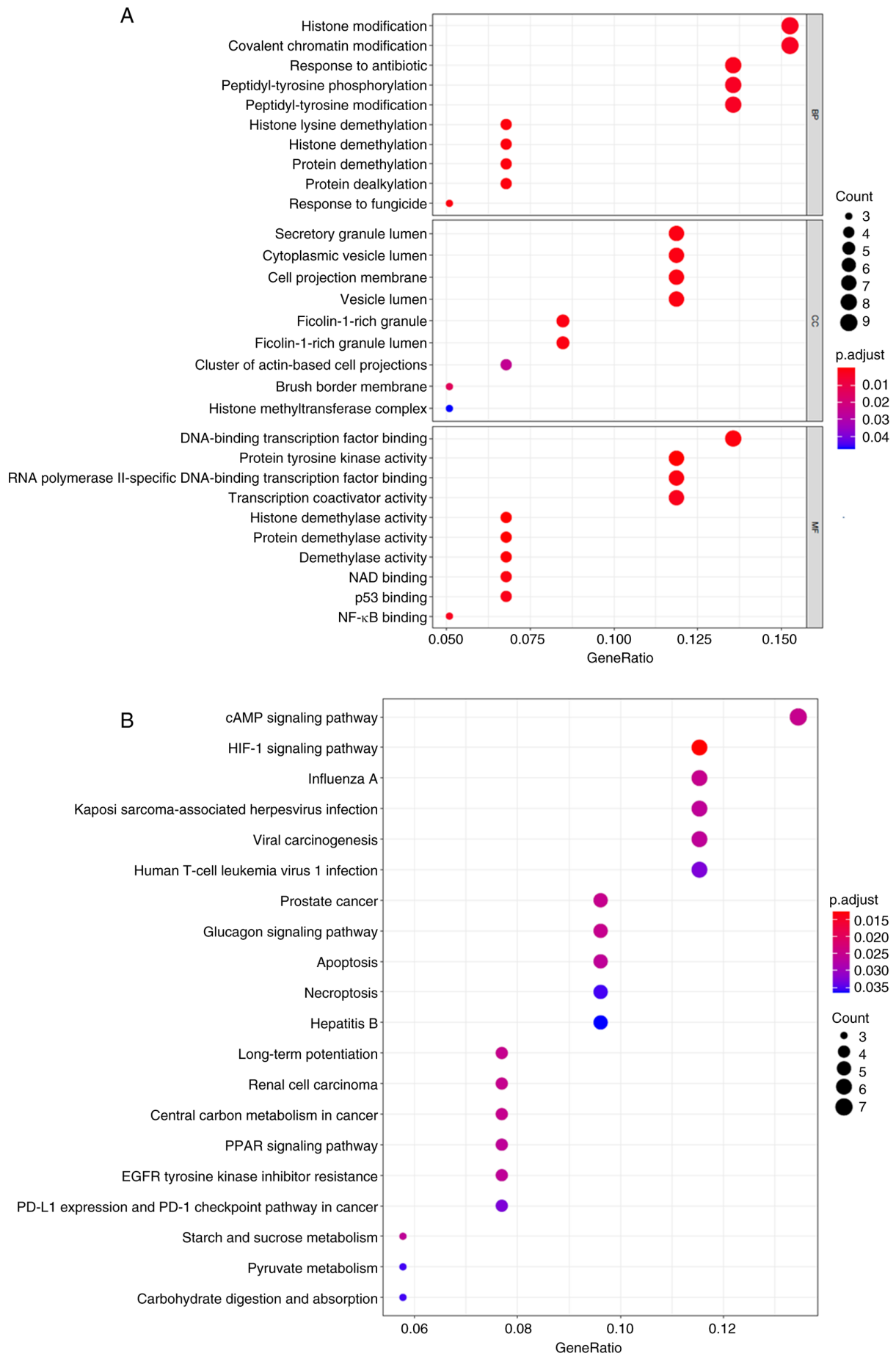


Figure 3. Functional enrichment analysis of 59 key genes. (A) GO analysis of core targets. (B) KEGG analysis of core targets. GO, Gene Ontology; KEGG, Kyoto Encyclopedia of Genes and Genomes.



Table II. Affinity score of potential targets and compounds by molecular docking.

Target	Compound	Affinity (kcal/mol)
EP300	4,4'-Dihydroxydiphenyl methane	-7.69
KDM6B	4,4'-Dihydroxydiphenyl methane	-8.04
HSP90AB1	4,4'-Dihydroxydiphenyl methane	-8.83
CREBBP	4,4'-Dihydroxydiphenyl methane	-8.12
EP300	Protocatechuic aldehyde	-5.49
KDM6B	Protocatechuic aldehyde	-5.04
HSP90AB1	Protocatechuic aldehyde	-5.93
CREBBP	Protocatechuic aldehyde	-5.41

EP300, E1A binding protein p300; KDM6B, lysine demethylase 6B; HSP90AB1, heat shock protein 90  $\alpha$  family class B member 1; CREBBP, CREB binding protein.

observed using the thioflavin-S fluorescence method. The transgenic strain CL2006 used in this experiment expressed the A $\beta$  protein fragment related to the development of AD. These worms showed expression and aggregation of A $\beta$  in muscle, leading to progressive paralysis. CL2006 was stained with triterpenes for A $\beta$  at the end of DM and PA treatment (green fluorescent labeling). The fluorescence image of the head area of CL2006 nematodes showed that compared with untreated worms (negative control), A $\beta$  deposition in those treated with 0.5 mM DM or 0.25 mM PA significantly decreased. The wild N2 strain exhibited no A $\beta$  deposition in any part of the animal (Fig. 6A). These results indicated that both DM and PA inhibit the aggregation and deposition of A $\beta$  in muscle cells of transgenic worms (Fig. 6B).

*Effects of DM and PA on gene expression in C. elegans.* Based on the results of network pharmacology and molecular docking, the regulatory effects of two active components of DM and PA with the core targets EP300, HSP90AB1, KDM6B and CREBBP were analyzed and verified using RT-qPCR. In *C. elegans*, the gene homologue of EP300 and CREBBP is CBP-1, that for KDM6B is JMJD3.1, and that for HSP90AB1 is HSP90 (35-37). Therefore, *CBP-1*, *JMJD3.1* and *HSP90* were examined. Compared with the control group, the expression levels of *HSP90* in the DM and PA groups were significantly increased ( $P < 0.01$ ) (Fig. 7). There was no significant effect on the expression levels of *CBP-1* in the DM or PA group. *JMJD3.1* was upregulated in the DM group ( $P < 0.01$ ).

## Discussion

In the present study, the combined power of network pharmacology and GEO were utilized to analyze the effects of GEB in AD. Firstly, a regulatory network of 31 active constituents and 59 key targets was constructed, and it was revealed that most compounds in GEB have overlapping targets and synergistic effects, suggesting that GEB has the capacity for multi-component and multi-target treatment of diseases, which is consistent with the concept of diseases

having multiple pathogenic factors and complex pathogenesis. In the network diagram 'drug-compound-target-AD', the two components with the highest degree values were DM and PA, strongly indicating that they have potential anti-AD activity. Most previous studies on the anti-AD effects of GEB focused on extracts and gastrodin, while DM and PA have not been investigated. New components in GEB for the treatment of AD may be identified (38,39).

GO analysis revealed that GEB may be associated with the biological process of regulating epigenetic histone modification (40). KEGG analysis showed that GEB may be associated with the cAMP signaling pathway that regulates the accumulation of A $\beta$  and neuronal apoptosis (41). Among the 59 key targets, five core targets were obtained through PPI: GAPDH, EP300, HSP90AB1, KDM6B and CREBBP. GAPDH was excluded as it was used as the internal reference. Among the four remaining proteins, HSP90AB1 is a stress-induced heat shock protein (HSP). HSPs can protect neurons by preventing protein misfolding to ensure proteome homeostasis and play a role in resisting oxidative stress and inhibiting apoptosis (42,43). HSP90AB1 is significantly downregulated in AD patients (44). Some studies suggest that HSP90AB1 is closely linked to astrocytes. A $\beta$  and tau proteins may be degraded by HSP90AB1 through autophagy (45,46). KDM6B is a specific histone 3 lysine 27 (H3K27) demethylase. KDM6B regulates the deposition of zebrafish glial cells by regulating the expression of chemokine, Wnt and FGF signaling pathway genes (47). In addition, KDM6B serves as an effective target for black chokeberry ethanolic extract to inhibit A $\beta$ -induced neuronal cell death (48). EP300 is a major acetylase involved in tau protein aggregation and neurodegeneration in AD (49). A previous study revealed that histone acetyltransferase, P300, can prevent and treat AD by regulating acetylation of AD-related gene promoters such as PS1 and BACE1 (50). CREBBP is an acetylated histone that affects age-related memory loss (51). The inhibition of CREBBP exerts an anti-inflammatory effect. Furthermore, studies have shown that CCC protects nerve cells and ameliorates cognitive impairment in an AD mouse model by regulating CREBBP (52). CREBBP is therefore considered an attractive target in drug design and development (53). In future studies, the regulatory effects of DM and PA on core targets will be examined through molecular docking and other experiments.

Among the pathological mechanisms of AD, that of A $\beta$  deposition is a hot research topic, and inhibiting A $\beta$  plaque aggregation is an effective strategy for preventing and treating AD (54). *C. elegans* is a classic model organism for studying AD and plays an important role in drug screening (55). There are numerous AD transgenic *C. elegans* lines (56,57), which exhibit a number of advantages such as a short life cycle, easy culture and high gene homology (58). Transgenic *C. elegans* can directly produce A $\beta$  plaques, which renders the observation and research of A $\beta$  convenient (59). In the present study, it was determined that both DM and PA effectively delayed the paralysis phenotype and inhibited A $\beta$  deposition in *C. elegans*. DM and PA exhibited similar efficacies, indicating that they directly inhibit A $\beta$  aggregation. Both DM and PA belong to the phenolic components of GEB. Consistent with a previous study, including p-hydroxybenzyl alcohol, they can inhibit the deposition of A $\beta$  in *C. elegans*, exert anti-aging and



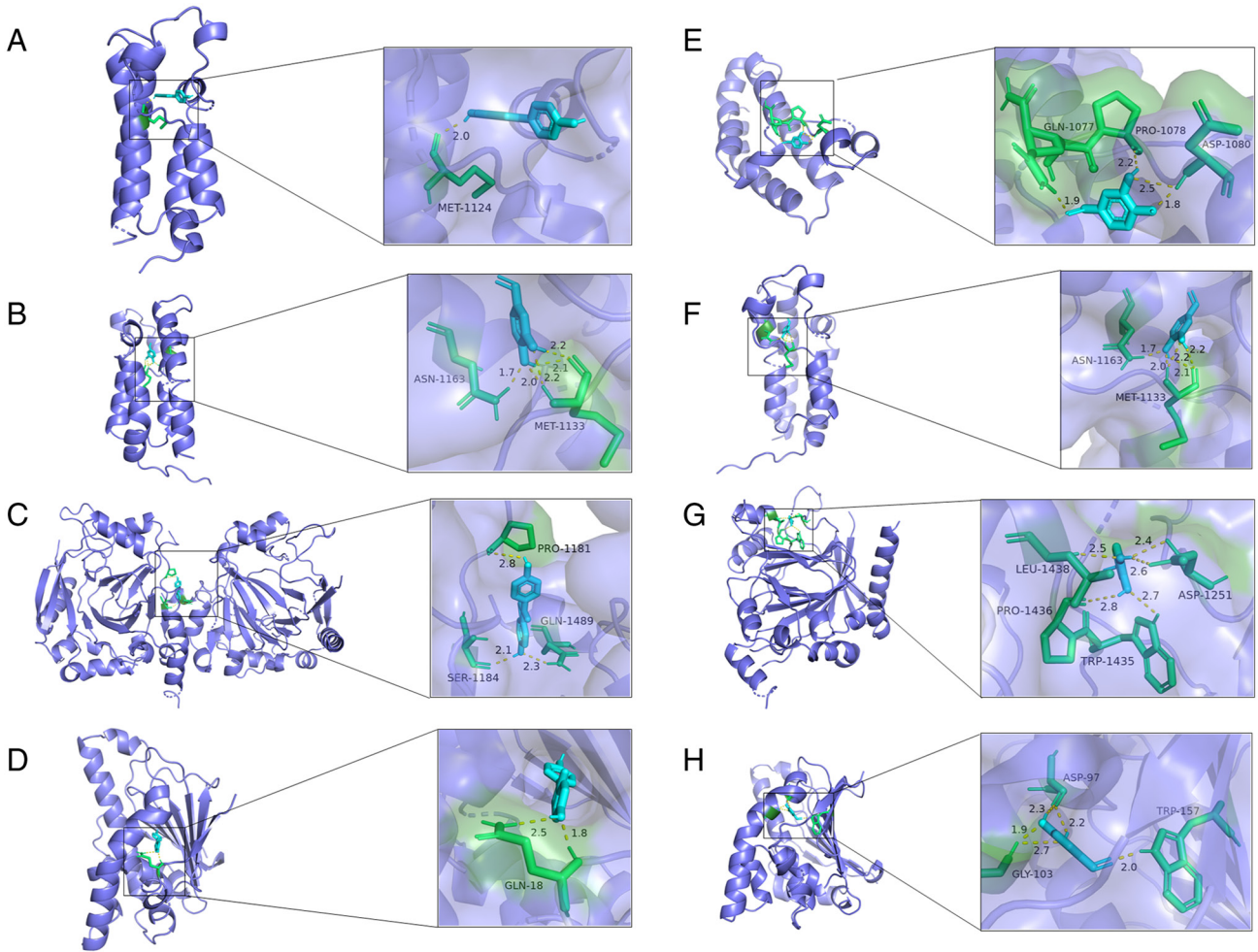


Figure 4. Molecular docking of core genes. (A) EP300-4,4'-dihydroxydiphenyl methane; (B) CREBBP-4,4'-dihydroxydiphenyl methane; (C) KDM6B-4,4'-dihydroxydiphenyl methane; (D) HSP90AB1-4,4'-dihydroxydiphenyl methane; (E) EP300-protocatechuic aldehyde; (F) CREBBP-protocatechuic aldehyde; (G) KDM6B-protocatechuic aldehyde; and (H) HSP90AB1-protocatechuic aldehyde.

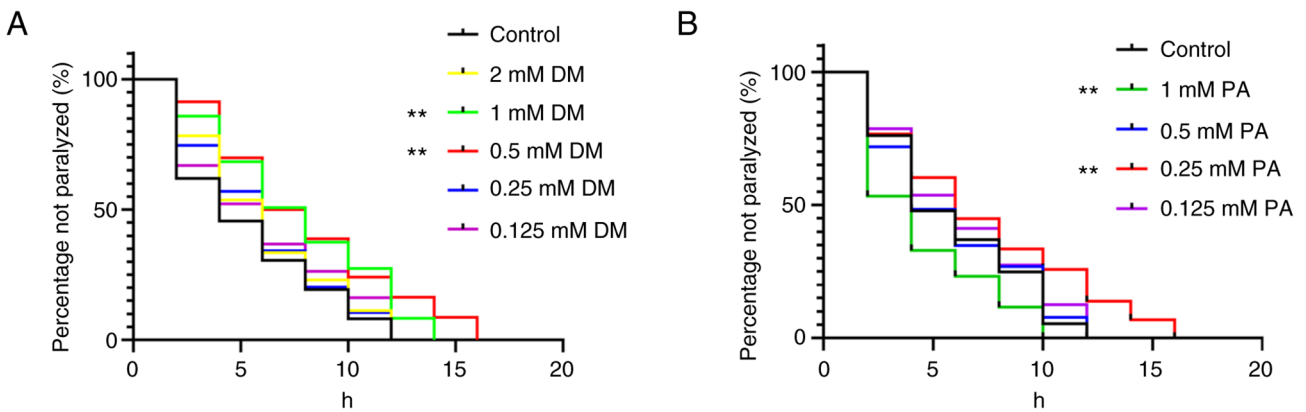


Figure 5. Effects of two components of GEB on paralysis of *C. elegans*. (A) 4,4'-Dihydroxydiphenyl methane and (B) protocatechuic aldehyde. The curve shows the process of paralysis induced by Aβ in transgenic *C. elegans* CL4176 (at least 80 worms were assessed in each group, and the experiment was conducted >3 times); \*\*P<0.01 vs. the control group. DM, 4,4'-dihydroxydiphenyl methane; PA, protocatechuic aldehyde.

antioxidative effects in *C. elegans*, as well as exert anti-AD biological activities (14). Notably, RT-qPCR revealed that both DM and PA regulate the expression of the heat shock protein HSP90, but have no impact on CBP-1. Only DM positively regulated JMJD3.1. Collectively, these findings suggest that

DM and PA may have therapeutic potential for AD, and can serve as focal points of future studies of GEB.

There are some limitations to the present study. The network pharmacology approach is based on reported components and targets. There may be more disease targets and components

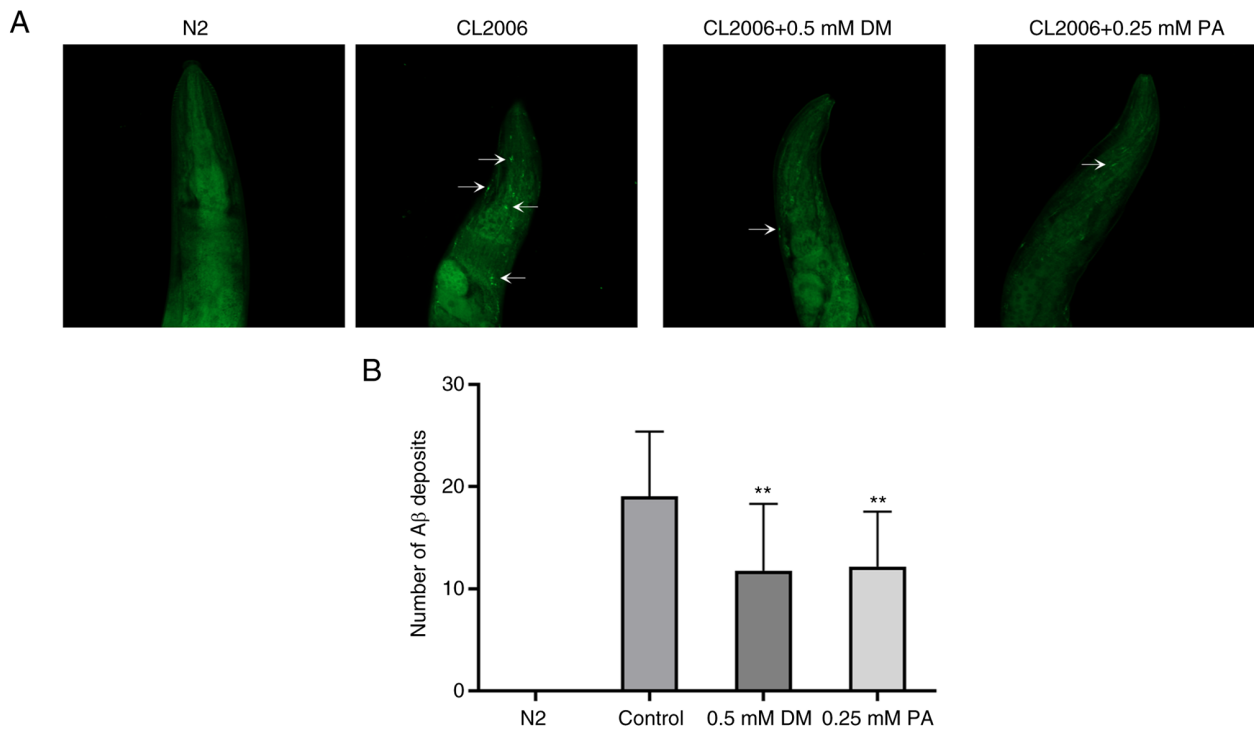


Figure 6. Effect of DM and PA on A $\beta$  aggregation in N2 and CL2006 *C. elegans*. (A) The fluorescence images were observed in N2 and CL2006 *C. elegans* after thioflavin S staining using a laser scanning confocal microscope (magnification, x200). (B) Deposition quantity of A $\beta$  in *C. elegans*; (at least 15 worms were assessed in each group, and data are presented as the mean  $\pm$  standard error of the mean). \*\*P<0.01 vs. the control group. DM, 4,4'-dihydroxydiphenyl methane; PA, protocatechuic aldehyde.

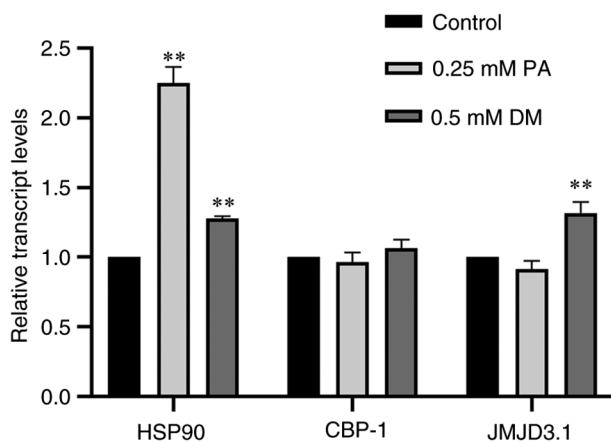


Figure 7. Regulation of DM and PA on the core target of *C. elegans*. Data are presented as the mean  $\pm$  standard error of the mean (n=3). \*\*P<0.01 vs. the control group. DM, 4,4'-dihydroxydiphenyl methane; PA, protocatechuic aldehyde.

that have yet to be discovered and the composition of GEB is complex, and therefore, network pharmacology may not fully reflect the effect of GEB in AD. Furthermore, studies using other animals, such as mice and rats, are required to better model the therapeutic actions of DM and PA in AD. In future studies, the anti-AD effect of DM and PA, two active components of GEB, will be further explored and the mechanism in combination with animal models such as rats and mice will be studied, in order to obtain data that may be clinically used.

In conclusion, network pharmacology identified two core components in GEB, DM and PA, and the core targets,

KDM6B, HSP90AB1, EP300 and CREBBP. Molecular docking revealed that DM and PA stably bound to the four core targets. DM (5 mM) and PA (0.25 mM) significantly delayed paralysis and inhibited the accumulation and deposition of A $\beta$  plaques. Both DM and PA upregulated the core target gene HSP90AB1, while DM upregulated KDM6B. DM and PA may be therapeutic candidates for AD.

#### Acknowledgements

Not applicable.

#### Funding

The present study was supported by the National Natural Science Foundation of China (grant no. 81960733), the Open Project of Yunnan Key Laboratory of Dai and Yi Medicines (grant no. 202210ZD2206), the Xingdian Talent Support Program-Special for Young Talent (2022), the National Administration of Traditional Chinese Medicine High-level Key Discipline Construction Project 'Dai Medicine'.

#### Availability of data and materials

The datasets used and/or analyzed during the current study are available from the corresponding author on reasonable request.

#### Authors' contributions

XS, YL and XD made considerable contributions to the experimental design, statistical data analysis and English

language editing. XD and LY are responsible for drafting the manuscript and revising it for important intellectual content. XS and LY confirm the authenticity of all the raw data. All authors read and approved the final manuscript.

### Ethics approval and consent to participate

Not applicable.

### Patient consent for publication

Not applicable.

### Competing interests

The authors declare that they have no competing interests.

### References

- Solanki I, Parihar P and Parihar MS: Neurodegenerative diseases: From available treatments to prospective herbal therapy. *Neurochem Int* 95: 100-108, 2016.
- Kent SA, Spires-Jones TL and Durrant CS: The physiological roles of tau and A $\beta$ : implications for Alzheimer's disease pathology and therapeutics. *Acta Neuropathol* 140: 417-447, 2020.
- de Caires S and Steenkamp V: Use of Yokukansan (TJ-54) in the treatment of neurological disorders: A review. *Phytother Res* 24: 1265-1270, 2010.
- The Pharmacopoeia Commission of PRC. Pharmacopoeia of the People's Republic of China. Volume 1. 10th Edition. China Medical Science and Technology Press, Beijing, pp58-59, 2015.
- Lin YE, Lin CH, Ho EP, Ke YC, Petridi S, Elliott CJ, Sheen LY and Chien CT: Glial Nrf2 signaling mediates the neuroprotection exerted by *Gastrodia elata* Blume in Lrrk2-G2019S Parkinson's disease. *Elife* 10: e73753, 2021.
- Kim HJ, Moon KD, Lee DS and Lee SH: Ethyl ether fraction of *Gastrodia elata* Blume protects amyloid beta peptide-induced cell death. *J Ethnopharmacol* 84: 95-98, 2003.
- Park YM, Lee BG, Park SH, Oh HG, Kang YG, Kim OJ, Kwon LS, Kim YP, Choi MH, Jeong YS, *et al*: Prolonged oral administration of *Gastrodia elata* extract improves spatial learning and memory of scopolamine-treated rats. *Lab Anim Res* 31: 69-77, 2015.
- Wang D, Wang Q, Chen R, Yang S, Li Z and Feng Y: Exploring the effects of *Gastrodia elata* Blume on the treatment of cerebral ischemia-reperfusion injury using UPLC-Q/TOF-MS-based plasma metabolomics. *Food Funct* 10: 7204-7215, 2019.
- Lu KH, Ou GL, Chang HP, Chen WC, Liu SH and Sheen LY: Safety evaluation of water extract of *Gastrodia elata* Blume: Genotoxicity and 28-day oral toxicity studies. *Regul Toxicol Pharmacol* 114: 104657, 2020.
- Manavalan A, Ramachandran U, Sundaramurthi H, Mishra M, Sze SK, Hu JM, Feng ZW and Heese K: *Gastrodia elata* Blume (tianma) mobilizes neuro-protective capacities. *Int J Biochem Mol Biol* 3: 219-241, 2012.
- Ramachandran U, Manavalan A, Sundaramurthi H, Sze SK, Feng ZW, Hu JM and Heese K: Tianma modulates proteins with various neuro-regenerative modalities in differentiated human neuronal SH-SY5Y cells. *Neurochem Int* 60: 827-836, 2012.
- Zhang JS, Zhou SF, Wang Q, Guo JN, Liang HM, Deng JB and He WY: Gastrodin suppresses BACE1 expression under oxidative stress condition via inhibition of the PKR/eIF2 $\alpha$  pathway in Alzheimer's disease. *Neuroscience* 325: 1-9, 2016.
- Liu ZH, Hu HT, Feng GF, Zhao ZY and Mao NY: Protective effects of gastrodin on the cellular model of Alzheimer's disease induced by Abeta25-35. *Sichuan Da Xue Xue Bao Yi Xue Ban* 36: 537-540, 2005 (In Chinese).
- Liu Y, Lu YY, Huang L, Shi L, Zheng ZY, Chen JN, Qu Y, Xiao HT, Luo HR and Wu GS: Para-hydroxybenzyl alcohol delays the progression of neurodegenerative diseases in models of *Caenorhabditis elegans* through activating multiple cellular protective pathways. *Oxid Med Cell Longev* 2022: 8986287, 2022.
- Ding Y, Bao X, Lao L, Ling Y, Wang Q and Xu S: p-Hydroxybenzyl alcohol prevents memory deficits by increasing neurotrophic factors and decreasing inflammatory factors in a mice model of Alzheimer's disease. *J Alzheimers Dis* 67: 1007-1019, 2019.
- Mishra M, Huang J, Lee YY, Chua DSK, Lin X, Hu JM and Heese K: *Gastrodia elata* modulates amyloid precursor protein cleavage and cognitive functions in mice. *Biosci Trends* 5: 129-138, 2011.
- Hopkins AL: Network pharmacology. *Nat Biotechnol* 25: 1110-1111, 2007.
- Liang WS, Dunckley T, Beach TG, Grover A, Mastroeni D, Walker DG, Caselli RJ, Kukull WA, McKeel D, Morris JC, *et al*: Gene expression profiles in anatomically and functionally distinct regions of the normal aged human brain. *Physiol Genomics* 28: 311-322, 2007.
- Yang X, Guan Y, Yan B, Xie Y, Zhou M, Wu Y, Yao L, Qiu X, Yan F, Chen Y and Huang L: Evidence-based complementary and alternative medicine bioinformatics approach through network pharmacology and molecular docking to determine the molecular mechanisms of Erjing pill in Alzheimer's disease. *Exp Ther Med* 22: 1252, 2021.
- Li S and Zhang B: Traditional Chinese medicine network pharmacology: Theory, methodology and application. *Chin J Nat Med* 11: 110-120, 2013.
- Daina A, Michielin O and Zoete V: SwissTargetPrediction: Updated data and new features for efficient prediction of protein targets of small molecules. *Nucleic Acids Res* 47: W357-W364, 2019.
- Piñero J, Ramírez-Anguaita JM, Saüch-Pitarch J, Ronzano F, Centeno E, Sanz F and Furlong LI: The DisGeNET knowledge platform for disease genomics: 2019 update. *Nucleic Acids Res* 48: D845-D855, 2020.
- Piñero J, Bravo A, Queralt-Rosinach N, Gutiérrez-Sacristán A, Deu-Pons J, Centeno E, García-García J, Sanz F and Furlong LI: DisGeNET: A comprehensive platform integrating information on human disease-associated genes and variants. *Nucleic Acids Res* 45: D833-D839, 2017.
- Ritchie ME, Phipson B, Wu D, Hu Y, Law CW, Shi W and Smyth GK: limma powers differential expression analyses for RNA-sequencing and microarray studies. *Nucleic Acids Res* 43: e47, 2015.
- Otasek D, Morris JH, Bouças J, Pico AR and Demchak B: Cytoscape Automation: Empowering workflow-based network analysis. *Genome Biol* 20: 185, 2019.
- Kolde R: Pheatmap: Pretty Heatmaps. R Package Version. CRAN Repository, 2012.
- Yu G, Wang LG, Han Y and He QY: clusterProfiler: An R package for comparing biological themes among gene clusters. *OMICS* 16: 284-287, 2012.
- Morris GM, Huey R, Lindstrom W, Sanner MF, Belew RK, Goodsell DS and Olson AJ: AutoDock4 and AutoDockTools4: Automated docking with selective receptor flexibility. *J Comput Chem* 30: 2785-2791, 2009.
- Morris GM, Huey R and Olson AJ: Using AutoDock for ligand-receptor docking. *Curr Protoc Bioinformatics* 8: Unit 8.14, 2008.
- Yang Y, He Y, Wei X, Wan H, Ding Z, Yang J and Zhou H: Network pharmacology and molecular docking-based mechanism study to reveal the protective effect of salvianolic acid C in a rat model of ischemic stroke. *Front Pharmacol* 12: 799448, 2021.
- Chen XY, Liao DC, Sun ML, Cui XH and Wang HB: Essential oil of *acorus tatarinowii* Schott ameliorates A $\beta$ -induced toxicity in *Caenorhabditis elegans* through an autophagy pathway. *Oxid Med Cell Longev* 2020: 3515609, 2020.
- Zhi D, Wang D, Yang W, Duan Z, Zhu S, Dong J, Wang N, Wang N, Fei D, Zhang Z, *et al*: Dianxianning improved amyloid  $\beta$ -induced pathological characteristics partially through DAF-2/DAF-16 insulin like pathway in transgenic *C. elegans*. *Sci Rep* 7: 11408, 2017.
- DanQing L, YuJie G, ChengPeng Z, HongZhi D, Yi H, BiSheng H and Yan C: N-butanol extract of *Hedyotis diffusa* protects transgenic *Caenorhabditis elegans* from A $\beta$ -induced toxicity. *Phytother Res* 35: 1048-1061, 2021.
- Livak KJ and Schmittgen TD: Analysis of relative gene expression data using real-time quantitative PCR and the 2(-Delta Delta C(T)) method. *Methods* 25: 402-408, 2001.
- Williams K, Christensen J, Rappalber J, Nielsen AL, Johansen JV and Helin K: The histone lysine demethylase JMJD3/KDM6B is recruited to p53 bound promoters and enhancer elements in a p53 dependent manner. *PLoS One* 9: e96545, 2014.

36. Mathies LD, Lindsay JH, Handal AP, Blackwell GG, Davies AG and Bettinger JC: SWI/SNF complexes act through CBP-1 histone acetyltransferase to regulate acute functional tolerance to alcohol. *BMC Genomics* 21: 646, 2020.
37. Eckl J, Sima S, Marcus K, Lindemann C and Richter K: Hsp90-downregulation influences the heat-shock response, innate immune response and onset of oocyte development in nematodes. *PLoS One* 12: e0186386, 2017.
38. Ng CF, Ko CH, Koon CM, Xian JW, Leung PC, Fung KP, Chan HYE and Lau CBS: The aqueous extract of rhizome of *Gastrodia elata* protected drosophila and PC12 cells against beta-amyloid-induced neurotoxicity. *Evid Based Complement Alternat Med* 2013: 516741, 2013.
39. Fasina OB, Wang J, Mo J, Osada H, Ohno H, Pan W, Xiang L and Qi J: Gastrodin from *Gastrodia elata* enhances cognitive function and neuroprotection of AD mice via the regulation of gut microbiota composition and inhibition of neuron inflammation. *Front Pharmacol* 13: 814271, 2022.
40. Narayan P and Dragunow M: Alzheimer's disease and histone code alterations. *Adv Exp Med Biol* 978: 321-336, 2017.
41. Li H, Yang S, Wu J, Ji L, Zhu L, Cao L, Huang J, Jiang Q, Wei J, Liu M, *et al*: cAMP/PKA signaling pathway contributes to neuronal apoptosis via regulating IDE expression in a mixed model of type 2 diabetes and Alzheimer's disease. *J Cell Biochem* 119: 1616-1626, 2018.
42. Gorenberg EL and Chandra SS: The role of Co-chaperones in synaptic proteostasis and neurodegenerative disease. *Front Neurosci* 11: 248, 2017.
43. Ramos E, Romero A, Marco-Contelles J, López-Muñoz F and Del Pino J: Modulation of heat shock response proteins by ASS234, targeted for neurodegenerative diseases therapy. *Chem Res Toxicol* 31: 839-842, 2018.
44. Li J, Xu C, Zhang J, Jin C, Shi X, Zhang C, Jia S, Xu J, Gui X, Xing L, *et al*: Identification of miRNA-target gene pairs in the parietal and frontal lobes of the brain in patients with Alzheimer's disease using bioinformatic analyses. *Neurochem Res* 46: 964-979, 2021.
45. Gonzalez-Rodriguez M, Villar-Conde S, Astillero-Lopez V, Villanueva-Anguita P, Ubeda-Banon I, Flores-Cuadrado A, Martinez-Marcos A and Saiz-Sanchez D: Neurodegeneration and astrogliosis in the human CA1 hippocampal subfield are related to hsp90ab1 and bag3 in Alzheimer's disease. *Int J Mol Sci* 23: 165, 2021.
46. Jeong HO, Park D, Im E, Lee J, Im DS and Chung HY: Determination of the mechanisms that cause sarcopenia through cDNA microarray. *J Frailty Aging* 6: 97-102, 2017.
47. Tang D, Lu Y, Zuo N, Yan R, Wu C, Wu L, Liu S and He Y: The H3K27 demethylase controls the lateral line embryogenesis of zebrafish. *Cell Biol Toxicol* 29: 10.1007/s10565-021-09669-y, 2021.
48. Kim J, Lee KP, Beak S, Kang HR, Kim YK and Lim K: Effect of black chokeberry on skeletal muscle damage and neuronal cell death. *J Exerc Nutrition Biochem* 23: 26-31, 2019.
49. Min SW, Chen X, Tracy TE, Li Y, Zhou Y, Wang C, Shirakawa K, Minami SS, Defensor E, Mok SA, *et al*: Critical role of acetylation in tau-mediated neurodegeneration and cognitive deficits. *Nat Med* 21: 1154-1162, 2015.
50. Lu X, Deng Y, Yu D, Cao H, Wang L, Liu L, Yu C, Zhang Y, Guo X and Yu G: Histone acetyltransferase p300 mediates histone acetylation of PS1 and BACE1 in a cellular model of Alzheimer's disease. *PLoS One* 9: e103067, 2014.
51. Barral S, Reitz C, Small SA and Mayeux R: Genetic variants in a 'cAMP element binding protein' (CREB)-dependent histone acetylation pathway influence memory performance in cognitively healthy elderly individuals. *Neurobiol Aging* 35: 2881.e2887-2881.e2810, 2014.
52. Kim MJ, Park SY, Kim Y, Jeon S, Cha MS, Kim YJ and Yoon HG: Beneficial effects of a combination of curcuma longa L. and Citrus junos against beta-amyloid peptide-induced neurodegeneration in mice. *J Med Food* 25: 12-23, 2022.
53. Akinsiku OE, Soremekun OS and Soliman MES: Update and potential opportunities in CBP [Cyclic Adenosine Monophosphate (cAMP) Response Element-Binding Protein (CREB)-Binding Protein] research using computational techniques. *Protein J* 40: 19-27, 2021.
54. Scheltens P, De Strooper B, Kivipelto M, Holstege H, Chételat G, Teunissen CE, Cummings J and van der Flier WM: Alzheimer's disease. *Lancet* 397: 1577-1590, 2021.
55. Paul D, Chipurupalli S, Justin A, Raja K and Mohankumar SK: *Caenorhabditis elegans* as a possible model to screen anti-Alzheimer's therapeutics. *J Pharmacol Toxicol Methods* 106: 106932, 2020.
56. Link CD: Expression of human beta-amyloid peptide in transgenic *Caenorhabditis elegans*. *Proc Natl Acad Sci USA* 92: 9368-9372, 1995.
57. Fay DS, Fluet A, Johnson CJ and Link CD: In vivo aggregation of beta-amyloid peptide variants. *J Neurochem* 71: 1616-1625, 1998.
58. Morcos M and Hutter H: The model *Caenorhabditis elegans* in diabetes mellitus and Alzheimer's disease. *J Alzheimers Dis* 16: 897-908, 2009.
59. Zhu S, Li H, Dong J, Yang W, Liu T, Wang Y, Wang X, Wang M and Zhi D: Rose essential oil delayed Alzheimer's disease-like symptoms by SKN-1 pathway in *C. elegans*. *J Agric Food Chem* 65: 8855-8865, 2017.



This work is licensed under a Creative Commons Attribution-NonCommercial-NoDerivatives 4.0 International (CC BY-NC-ND 4.0) License.